Kopcansky, P.; Siposova, K.; Melnikova, L.; Bednarikova, Z.; Timko, M.; Mitroova, Z.; Antosova, A.; Haramus, V.M.; Petrenko, V.I.; Avdeev, M.V.; Gazova, Z.:

Destroying activity of magnetoferritin on lysozyme amyloid fibrils

In: Journal of Magnetism and Magnetic Materials (2014) Elsevier

DOI: 10.1016/j.jmmm.2014.10.017

Destroying activity of magnetoferritin on lysozyme amyloid fibrils

P. Kopcansky[1], K. Siposova[1], L. Melnikova[1], Z. Mitroova[1], V. M. Garamus[2], V. I. Petrenko[3,4], M. V. Avdeev[3], Z. Gazova[1]

[1]Institute of Experimental Physics, SAS, Watsonova 47, 040 01 Kosice, Slovakia
[4]Helmholtz-Zentrum Geesthacht: Centre for Materials and Coastal Research, Max-Planck-Street 1, 21502 Geesthacht, Germany
[3]Joint Institute for Nuclear Research, Joliot-Curie 6, 141980 Dubna, Moscow region, Russia
[4]Kyiv Taras Shevchenko National University, Volodymyrska Street 64, Kyiv, 01033 Ukraine

Abstract.

In the human body the protein amyloid aggregates, due to their deposition in specific tissues or organs, are associated with many serious diseases (diabetes mellitus, Alzheimer's disease, etc.). Recently, we have found that magnetite nanoparticles have ability to affect amyloid aggregatation of lysozyme and insulin [1][2]. In our study we examine effect of magnetoferritin (MFer), biocompatible magnetite nanoparticles, on lysozyme amyloid aggregates (LAA) associated with lysozyme systemic amyloidosis. The interference of LAA and MFer was investigated at ratios of LAA:MFer = 1:1 and 1:5 using small angle X-rays scattering technique (SAXS) and Thioflavin T fluorescence measurements (ThT assay). By controlled chemical synthesis magnetoferritin complexes with two loading factors (LF - number of iron atoms per one complex) of 168 (MFer(168)) and 532 (MFer(532)) were prepared. SAXS experiments indicate that presence of MFer caused structural changes of LAAs. Analysis of data obtained for solution containing LAA with MFer(532) (LAA:MFer = 1:5) clearly indicate decreasing of the lower limit of radius of gyration from 30 nm to 20 nm compare to lysozyme fibrils alone and almost non-effected structure of MFer complexes (Fig. 1). These results suggest reduction of LAA, probably due to the truncation of the LAA by MFer. The decreasing of the amount of LAA was observed also by ThT assay. The fluorescence intensities of LAA in presence of MFer(532) and MFer(168) was significantly decreased - 40% and 55% decay (ratio 1:1) and 50% and 62% decay (ratio 1:5). These data strongly support SAXS data assuming reduction of the LAA as results of their interaction with MFer.

The interaction between lysozyme amyloid aggregates (LAA) and biocompatible magnetite nanoparticles (magnetoferritin, MFer) have been investigated by Thioflavin T fluorescence

measurements (ThT assay), small-angle X-rays scattering (SAXS) and transmission electron microscopy (TEM). The influence of concentration and degree magnetite loading (loading factors) of MFer has been examined during LAA formation (inhibition) and after LAA formation (depolymerisation) experiments. Results suggest the reduction of LAA size in the case of high concentration and LF of added magnetoferritin during depolymerisation, probably due to the truncation of the LAA by MFer. Shell structure of MFer is observed in LAA/MFer mixtures.

Keywords: Magnetoferritin, magnetic nanoparticles, lysozyme amyloid aggregates, biological small-angle X-rays scattering, florescence spectroscopy, transmission electron microscopy.

1. Introduction

The conversion of normally soluble protein into fibrillar aggregates is of central importance for several diseases, including Alzheimer's and Parkinson's diseases or type II diabetes. The common feature of amyloid diseases is presence of amyloid deposits consisting mainly of aggregated poly/peptide typical for given disease [3-7].

Such degenerative diseases are closely related to disorder of normal metabolism of iron, associated with iron storage protein, ferritin [8]. Physiological ferritin (~ 12 nm in diameter) without disruption of normal storage function consists of protein shell, apoferritin, surrounding the mineral core of hydrated ferric phosphate complex [9]. Many studies have shown that mineral core of brain ferritin in patients with neurodegenerative diseases is partial transformed to magnetite/maghemite (Fe_3O_4/γ-Fe_2O_3), but it has not been established yet, if their creation is related to the origin of the neurodegenerative diseases or to their consequences [10]. The polycrystalline structure of such pathological ferritin may play an important role in the biochemical processes associated with the generation of protein aggregates [11]. For these reasons is very important to characterize the structure of protein aggregates in the presence of pathological ferritin *in vivo*, and in the presence of magnetoferritin *in vitro*, respectively, especially for the understanding the role of Fe_3O_4/γ-Fe_2O_3 formation in the development of neurodegenerative diseases. Magnetoferritin, synthetic derivate of ferritin, with magnetic iron core (Fe_3O_4/γ-Fe_2O_3), described for the first time by Mann and co-workers [11], represents useful model system for the study of its effect on protein aggregates.

Lysozyme was selected as a amyloidogenic protein to study interaction between MFer and amyloid aggregates in "*in vitro*" conditions. In our previous works, we have showed that magnetite nanoparticles are able to reduce amount of insulin and lysozyme aggregates in vitro [1, 2]. Mechanism of anti-aggregating (inhibiting and destroying) activity has not been fully determined yet and research in this field shows that it strongly depends on the size, surface and concentration of magnetic nanoparticles with different size, surface and concentration can affect protein amyloid aggregation differently . In present work the interaction between MFer and lysozyme amyloid aggregation was investigated by florescence spectroscopy, transmission electron microscopy and structure sensible SAXS methods. We have detected observed and analyzed conformational changes in the LAA structure after addition of MFer and distance size distribution p(r) with corresponding *ab initio* models using basic approach of SAXS data analysis. We have found thatwhich point that MFer is able to decrease degree of aggregation destroy and affectof amyloid fibrils formation in vitro.

2. Experimental methods

2.1. Chemicals

Ammonium ferrous sulfate hexahydrate ($(NH_4)_2Fe(SO_4)_2.6H_2O$), equine spleen apoferritin in 0,15 M NaCl, 3-[(1,1-dimethyl-2-hydroxy-ethyl)amino]-2, hen egg white lysozyme (lyophilized powder, L6876, ~50,000 units mg^{-1} protein), hydroxypropanesulfonic acid (AMPSO), hydrochlorid acid (HCl), sodium chloride (NaCl,) disodium hydrogen phosphate dodecahydrate $Na_2HPO_4.12H_2O$, , potassium thiocyanate (KSCN), sodium hydroxide (NaOH) and trimethylamine N-oxide (Me_3NO) were obained from SIGMA-Aldrich.

2.2 Preparation of magnetoferritin

Magnetoferritin was synthesized by incorporation of iron ions into apoferritin molecules in anaerobic conditions (N_2) at 65 °C and alkaline pH (0.05 M AMPSO buffered to pH 8.6 with 2 M NaOH). Two samples with loading factors of 168 and 532 were prepared. Loading factor represents the number of iron atoms per one apoferritin macromolecule. After the synthesis, these samples were freeze dried for 24 hours to obtain a powder. Finally, 100.00 $g.l^{-1}$ stock solutions were prepared by weighing and dissolving powders with accurate volume of demineralized water.

The loading factor (LF) of samples was determined spectrophotometrically using UV-VIS spectrophotometer SPECORD 40, Analyik Jena. Protein concentration was detected using standard Bradford method at wavelength (λ) 595 nm and amount of iron was measured after HCl/H_2O_2 oxidation and KSCN addition by light absorption of thiocyanate complex at λ = 400 nm.

2.3 Amyloid aggregation of lysozyme

Amyloid aggregates of lysozyme (LAA) were achieved by incubation of lysozyme (10 mg/ml) in 20 mM Na_2HPO_4 - acid citric buffer, in presence of 80 mM NaCl, pH 6.0 at 65°C, 1200 rpm for 2 hours. stockPresence of fibrils was confirmed by ThT fluorescence assay and transmission electron microscopy. Prepared LAA were diluted in phosphate buffer pH 6.0 to achieve of 2 $g.L^{-1}$ concentration.

2.4 Mixtures of LAAs and MFer for inhibition and depolymerisation expetriments

The interaction of the magnetoferritin with lysozyme amyloid aggregation was observed at two modes: i) Inhibition: to investigate effect of magnetoferritin on the fibrillization of lysozyme the two concentrations (2 and 10 gL^{-1}) of magnetoferrin and two LF (168 and 532) were added into the solution of native lysozyme (final concentration of 2 gL^{-1}) and exposed to the conditions inducing amyloid aggregation as described in part 2.3. ii) Depolymerisation: to investigate effect of the magnetoferritin on the mature lysozyme amyloid fibrils. The LAAs were incubated with MFer solutions at two weight ratios between LAAs:MFer 1:1 (2:2 gL^{-1}) and 1:5 (2:2 gL^{-1}) and LFs (168 and 532) at 37°C for 24 hours.

2.54 Thioflavin T (ThT) fluorescence assay

Formation of LAA was detected as a significant enhancement of the ThT fluorescence intensity in the presence of amyloid fibrils. ThT was added to the lysozyme samples (10 μM) in a final concentration of 2.00 $g.L^{-1}$ and incubated at 37°C 1 h. Measurements were carried out in semimicro-quartz cuvettes with 1 cm excitation light path using spectrofluorimeter (Shimadzu, type RFA-500). The excitation was set at 440 nm and the emission recorded at 485 nm. The slits were adjusted to 1.5 and 3.0 nm for the excitation and emission accordingly.

2.5 Interference of magneoferritin and lysozyme amyloid aggregation

The interaction of the magnetoferritin with lysozyme amyloid aggregation was observed at two modes: i) to investigate effect of magnetoferritin on the fibrillization of lysozyme the magnetoferrin was added into the solution of native lysozyme (final concentration of 2.00 $g.L^{-1}$) at two different concentrations - 2.00 and 10.00 $g.L^{-1}$and exposed to the conditions inducing amyloid aggregation as described in part Amyloid aggregation of lysozyme. Formation of amyloid aggregates was detected by ThT assay. ii) to investigate effect of the magnetoferritin on the mature lysozyme amyloid fibrils the fibrils were incubated with MFer at two weight ratios, 1:1 (2.00:2.00 $g.L^{-1}$) and 1:5 (2.00:10.00 $g.L^{-1}$), at 37°C for 24 hours. The amount of amyloid aggregates was observed by ThT assay.

conditions inducing amyloid aggregation as described in part Amyloid aggregation of lysozyme. The extent of inhibiting activity was determined by ThT assay.

2.6 Biological sSmall-angle X-ray scattering

Small-angle X-rays scattering measurements were performed at the P12 BioSAXS beamline of the European Molecular Biology Laboratory at the storage ring PETRA III of the Deutsche Elektronen Synchrotron (DESY, Hamburg, Germany) at 20°C using a Pilatus 2M detector (Dectris, Switzerland) and synchrotron radiation with a wavelength $\lambda = 0.1$ nm. The *q*-range (0.,05731- 3.,8 nm^{-1}75801) was calibrated using diffraction patterns of silver behenate. Experimental data were normalized to the transmitted beam intensity. A thin glass capillary with diemater of 1 mm column and sample volume 50 µl was were used during measurements including manual change and filling of capillaries. The solvent scattering was measured before sample scattering.. The experiment was performed in triplicate and the final scattering curve is average of three experimental curves. No measurable radiation damage of samples was determined during their 5 s exposure to X-rays. The final scattering curves were obtained by the manual subtraction of buffer scattering. In order to verify that no artifacts as a result of radiation damage occurred, all scattering curves of a recorded dataset were compared to a reference measurement (typically the first exposure) and finally integrated by automated acquisition program [Franke, D., A.G. Kikhney, and D.I. Svergun, *Automated acquisition and analysis of small angle X-ray scattering data.* Nuclear Instruments and Methods in Physics Research Section A: Accelerators, Spectrometers, Detectors and Associated Equipment, 2012. **689**: p. 52-59.]. The background scattering of the aqueous buffer was substractedsubtracted.

3. Results and discussion

3.1 Population of LAA fibrils from fluorescence data

The presence of LAA was detected by spectrofluorimeter as an increase of the fluorescence intensity that was not observed for lysozyme solution (Fig. 2).

The decreasing of the amount of LAA was observed by ThT assay. The fluorescence intensities of LAA in presence of MFer(532) and MFer(168) was significantly decreased - 40% and 55% decay (ratio 1:1) and 50% and 62% decay (ratio 1:5). The anti-amyloidal effect of MFer dispersion on LAA was studied *in vitro* by ThT fluorescence assay. The method is sensitive to the interaction between the dye and fibrils and allows detection of LAA amount reduction that is proportional to the fluorescence intensity in the presence of ThT. It was necessary for data quantification to measure pure MFer for which fluorescence signal was negligible.

Effect of MFer on prepared LAA was investigated after 24-hours incubation at 37°C using ThT assay. The fluorescence intensities were obtained for two various weight ratios of proteins LAA: MFer, i.e. 1:1 and 1:5 (Fig. 2 doplnit). The result . The fluorescence intensity of lysozyme fibrils in the presence of MFer(532) and MFer(168) was significantly decreased - 40% and 55% decay (ratio LAA:MFer = 1:1) and 50% and 62% decay (ratio 1:5) due to reduction of lysozyme amyloid aggregates amount. TheeductionDestroying of the fibrils, probably due to the truncation of the fibrils was as a result of the interactions between lysozyme fibrils and magnetoferritin.

3.2 Structure of initial LAA and MFer (SAXS and TEM)

The morphology of samples was observed by transmission electron microscopy (TEM) (Fig. 1 a.) b.) doplnit MFer a.) a ciste LAA b.)). TEM image has suggested typical shape and sizes of LAA with average diameter of…doplnit and spherical shape of magnetoferritin with $<D_{CORE}>$ ~ 4 nm.

SAXS data on Apoferritin and MFer (Fig. SAXS APO and MFer, please put here 3 curves APO, MFer 168 and 532) suggest some deviation from shell structure for MFer with LF 168 and 532 to compare with shell structure of Apofferitin. Analysis has been done by

Indirect Fourier Transformation (IFT) approach with further ab intio modelling (Fig. Ab initio models of APO and MFer).

The SAXS curve of LAA indicates to large aggregates which size is larger than observation window and slope of 3.25 suggests the presence of compact core and fractal surface. Here IFT should be used with caution and just point on lower size limit of studied aggregates.

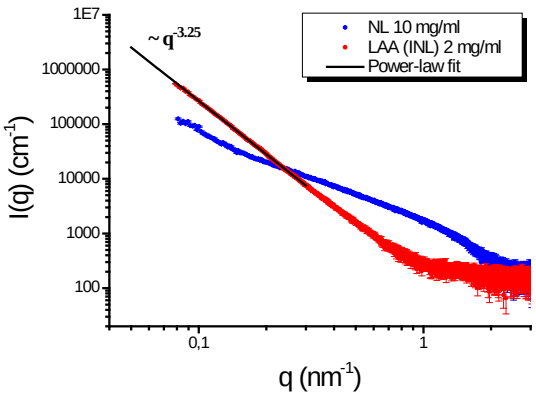

Fig. SAXS of LAA Experimental scattering SAXS curves of LAA(DNL) a.). Native lysozyme (NL) and lysozyme amyloid aggregates (LAA/INL) b.). LAA curve was modeled with the power-law ~ $q^{-3.25}$ that corresponds to fractal surface characterised by a fractal dimension D_s = 2.75

To characterize the effect of different amount of loaded iron on the properties of magnetoferritin the SAXS experiments were carried out.

3.1 3 Depolymerisationsing activity. Magnetoferritin represents system consisting of iron nanoparticles inserted into protein envelope formed by apoferritin. Due to the fact, that ferritin is naturally occurring in human body, the magnetoferritin should be highly biocompatible and eliminates the toxicity of the free iron. Moreover, the controlling loading of the iron into apoferritin allows the preparation of magnetoferritins with different amount of magnetite nanoparticle inside of protein envelope which can affect the interaction of MFer with lysozyme amyloid aggregation.

The specific conditions of the chemical synthesis were used to prepare magnetoferritin with different amount of iron loading per one apoferritin????? molecule (loading factor=LF). The definite LF of magnetoferritin samples, 168 and 532, was determined spectrophotometrically.

Structural changes due to (depolymerization and inhibition) were obtained by For comparison SAXS data with all mixtures after incubation (depolymerization and inhibition experimental scattering curves), with “theoretical” curves which have were plottedhave been calculated as

$$I_{(theor)} = \varepsilon_{LAA} * I_{(LAA)} + \varepsilon_{MFer} * I_{(MFer)} \quad (1)$$

where $I_{(LAA)}$ is scattering curve of initial fibrils solution and $I_{(MFer)}$ of initial magnetoferritin solution, ε are corresponding concentrations.

as q versus $I_{(theor)}$ dependence as is shown in Fig 8 a.) with correscopning power law lines at small q-region. $I_{(theor)}$ included volume fraction ε of the sample and intensities of two different materials, according to the equation:

$$I_{(theor)} = \varepsilon_{LAA} * I_{(LAA)} + \varepsilon_{MFer} * I_{(MFer)}$$

Depolymerization experiments wereas performed by mixing of MFer in alkaline pH 8.6 and LAA in pH 6.0. The outher negative charge of magnetoferritin biomacromolecules in the mixture leads to the electrostatic Coulomb repulsion between magnetoferritins. The scattering curves in comparison with theoretical have shown that MFer biomacromolecules in the mixture is homogenously dispersed between lysozyme amyloid aggregates and these two system do not interact with each otherare almost uneffected. Slopes at the small q-region have shown minimal differences in comparison with theoretical slopes Fig 8 a.). Depolymerization effect was observed only in the case of high fraction of MFer (mixture 1:5) and LF 532 from PDD functions at weight ratio 1:5 and MFer with higher LF 532 only (Fig. 8a b.)) i.e., the decreasing of scattering intensity at low q range and more pronounce maximum at large q point on lower contribution from LAA fibrils as it is expetected by ideal mixing of initial component. Further IFT analysis gives us the shape of p(r) functions (Fig. 8b) for initial component and solution after depolymerization which support the presence of MFer aggregates and decreasing the size of LAA fibrils (smaller maximal r and movement of second maximum of p(r) to lower r). . In this case we should consider different pH values of both systems (LAA and MFer) and comparisons with theoretical curves only. The confomation change of very stable lysozyme amyloid aggregates at higher pH value > 6 in such mixture is very improbable, but structure of MFer coat (apoferritin) is very unstable at diffetrent pH values as was demonstrated in work by Kim et al. [13]. Magnetoferritin dispersion also, due to its unseparation, contains salts, small amount of Fe ions and secondary product of synthesis, which could distort results. If we neglect these facts, SAXS experiment give strong conclusion as it was in the case of fluorescence experiments, i.e. depolymerization effect of MFer(532) with concentration 10 $g.L^{-1}$ in mixture.

3.2 Inhibiting activity

SAXS data on inhibition samples do not show the presence of any LAA fibrils only scattering from MFer is observed (Figure 9 a and b).

During the LAA formation MFer was added to the soluble lysozyme before initiation of aggregation. Detected inhibiting activity of MFer was observed by decreasing fluorescence intensity similar to depolymerization experiment. To study morphology of both mixtures types of LAA and MFer, for depolymerization and inhibition, we used TEM microscopy.. In Fig. 3 the typical imagination of such mixture is observed and visible LAA reduction in comparison with pure LAA from Fig 1 b.). The result confirms inhibition effect of MFer on LAA.

Biological small-angle X-ray scattering was applied for aqueous dispersions of apoferritin (Apof), magnetoferritin (MFer) with two loading factors (LF) 168 and 532 and two different concentrations 2.00 and 10.00 $g.L^{-1}$, native lysozyme (NL) and lysozyme amyloid aggregates (LAA). Experimental scattering curve of apoferritin is characterized by minima and maxima corresponding to the typical core-shell structure (Fig. 4). The structure is more compact, if the biomacromolecule of apoferritin is loaded by iron in the case of MFer (Fig. 5 a.) b.)). Presence of an uncertain amount of fibrils and an effect of interparticle interactions are more visible in MFer 532 with 10 mg/ml at low q region (Fig. 5 b.)). Fitting parameters used for core-shell models assembly are collected in Tab. 1. The pair-distance distribution (PDD) function of basic materials, containing information about the real space representation of particle shape, is shown in Fig. 6 a.) b.). Parameters used for the PDD fitting were obtained by the Indirect Fourier Transformation using WIFT software in narrow q range typical for monomers (Tab. 2). *Ab initio* model at Fig. 7 a.) is typical for apoferritin and models for both magnetoferritins (LF 168 and 532) have shown partial shell destruction (Fig. 7 b.) c.)).

Inhibition experiments were performed because of finding if MFer is able to slow LAA formation. Pure MFer (pH 8.6) and pure NL (pH 6.0) were mixed and heated at 65°C together with constant stiring (1200rpm). Some experimental inhibition curves with hight mass ratio of MFer, in comparison with depolymerization curves, correspond to the core-shell structure (Fig. 9 a.), b.)). This fact guides to think that MFer with its uncovered redox surface according to partial destruction of the shell (Fig 7. b.) c.)) bounds to native lysozyme or LAA and causes some structural changes, not visible by SAXS according to samples sedimentation. Therefore we see some part of apoferritin shell only from SAXS data (Fig. 9 a.) b.)).

4. Conclusions

We studied in this research disassembly of lysozyme amyloid aggregates and inhibition of their formation by magneoferritin with florescence spectroscopy combined with transmission electron microscopy and biological Small-angle neutron scattering. These results have shown that magneoferritin with loading factor 532 was able to destroy lysosyme amyloid aggregates at weight ratio 1:5.

Acknowledgemens

This work was supported by the Slovak Scientific Grant Agency VEGA (projects No. 0041, 0045, 0181), by the European Structural Funds, projects NANOKOP No. 26110230061 and 26220120021, PHYSNET No. 26110230097, APVV 0171–10 (METAMYLC) and M-ERA.NET MACOSYS. Dr. Clement Blanchet (EMBL) is acknowledged for help during SAXS measurements.

References

[1] A. Bellova et al. 2010 Nanotechnology 21 065103

[2] K. Siposova et al. 2012 Nanotechnology 23 055101

[3] J. D. Sipe. 2005 Amyloid Proteins (Weinheim: Wiley–VCH)

[4] L. Obici, et al. 2005 Clinical Biochim. Biophys. Acta 1753 11

[5] Khlistunova, et al. 2006 J. Biol. Chem. 281 1205.

[6] B. Granel, et al. 2006 Medicine (Baltimore) 85 66

[7] E. D. Roberson, et al. 2007 Science 316 750

[8] A. Friedman, et al. 2011 Parkinsonism Relat. Disord.17 423

[9] N. D. Chasteen and P. M. Harrison. 1999 J. Struct. Biol. 126 182

[10] J. L. Kirschvink, et al. 1992 Proc. Natl. Acad. Sci. USA 89 7683.

[11] J. Dobson. 2001 FEBS Letters. 496

[12] F. C. Meldrun, B. R. Heywood and S. Mann. 1992 Science 257 522

[13] M. Kim et al. 2011 Biomacromolecules 12 1629

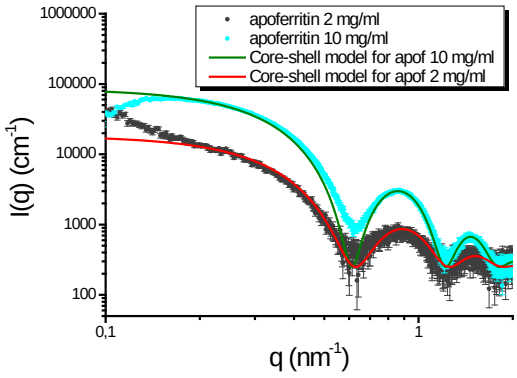

Fig. 4 Experimental scattering SAXS curves of apoferritin with two different concentrations 2 and 10 mg/ml in comparison with corresponding core-shell models

a.) b.)

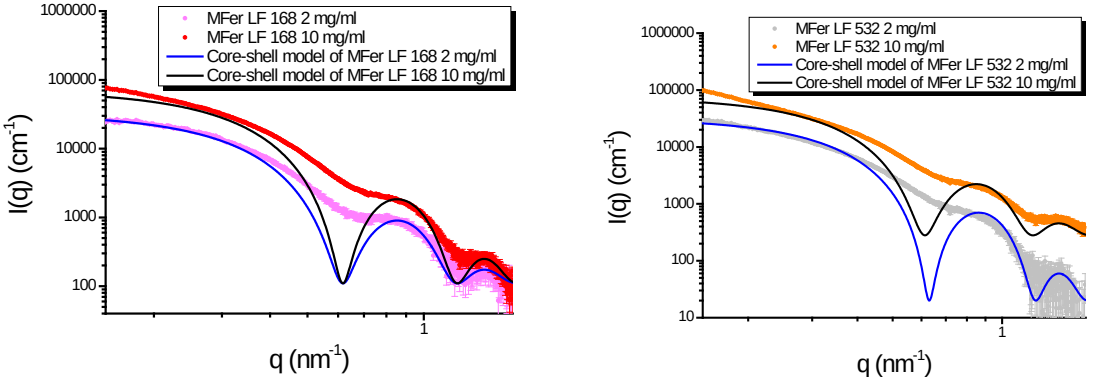

Fig. 5 Experimental scattering SAXS curves of magnetoferritin with two different concentrations 2 and 10 mg/ml and two LFs 168 and 532 in comparison with corresponding core-shell models

Tab. 1 The best fitting values used for the core-shell model of experimental SAXS data

Sample	c_{mass} [mg/ml]	R_{OUTER} (nm)	R_{INNER} (nm)	I_0 (cm^{-1})	I_{BG} (cm^{-1})
apof	2	6.00	3.80	0.18E+5	0.25E+3
	10	6.25	3.80	0.85E+5	0.25E+3
MFer(168)	2	6.50	3.30	0.32E+5	0.11E+3
	10	6.50	3.30	0.70E+5	0.11E+3
MFer(532)	2	6.50	3.00	0.32E+5	0.20E+2
	10	6.50	3.40	0.75E+5	0.28E+2

a.) b.)

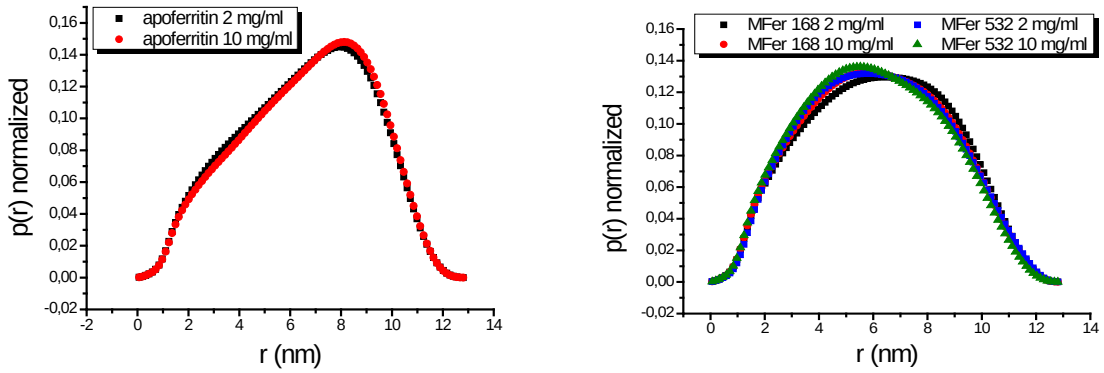

Fig. 6 PDD graphs of apoferritin and magnetoferritin and their comparisons

Tab. 2 Fitting parameter using for PDD functions obtained by WIFT software

Sample	c_{mass} [mg/ml]	R_G (nm)	I_0 (cm^{-1})	D_{max} (nm)	λ	q - range (nm^{-1})
Apof	2	5.0347 ± 0.0102	0.11374E+5 ± 131.9	13.00	1.0	0.4011 - 1.9828
	10	5.0867 ± 0.0014	0.67762E+5 ± 166.1	13.00	1.0	0.4011 - 1.9828
MFer LF 168	2	4.8063 ± 0.0070	0.22483E+5 ± 137.8	13.00	1.0	0.4011 - 1.9828
	10	4.7262 ± 0.0026	0.53546E+5 ± 115.0	13.00	1.0	0.4011 - 1.9828
MFer LF 532	2	4.7324 ± 0.0053	0.20731E+5 ± 92.9	13.00	1.0	0.1260 - 1.4671
	10	4.6333 ± 0.0031	0.50228E+5 ± 125.6	13.00	1.0	0.4011 - 1.9828

a.) b.) c.)

Fig. 7 Ab initio models of apoferritin a.), MFer 168 b.) and MFer 532 c) with protein concentration of 10 mg/ml by DAMMIF/RASWIN using PDD function (from Fig. 9)

a.) b.)

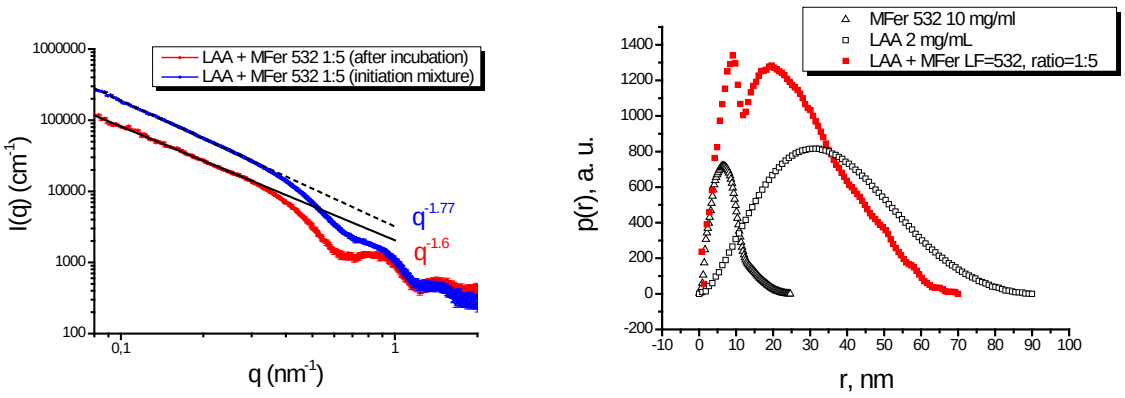

Fig. 8 Theoretical and experimental averaged SAXS curve of mixture LAA + MFer LF 532 (1:5) a.). The initial parts of curves were modeled with the power-law, $q^{-1.77}$ and $q^{-1.6}$ coresponds to a mass fractal with dimension D_s = 1.77 and 1.6. PDD functions of mixture in comparison withz pure LAA and MFer b.).

a.) b.)

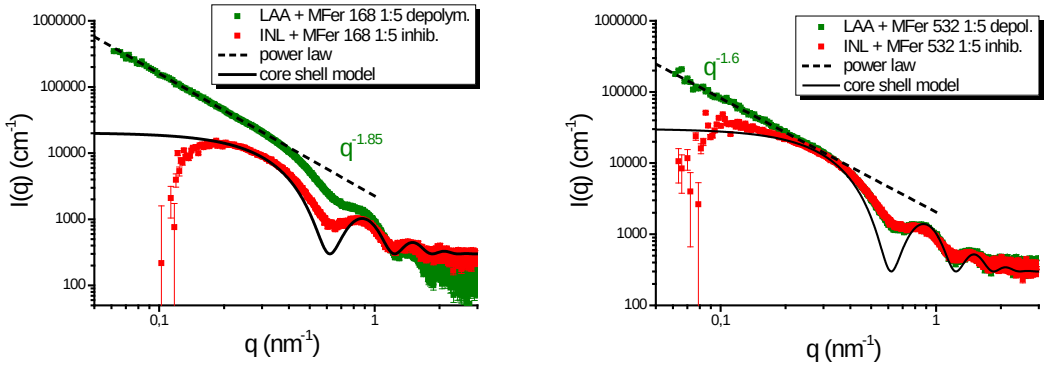

Fig. 9 Comparison of experimental SAXS curves of depolymetrization and inhibition mixtures with core-shell models